

# The dynamical stability of reverberatory neural circuits

Jesper Tegnér<sup>1,2,3</sup>, Albert Compte<sup>1,4</sup>, Xiao-Jing Wang<sup>1</sup>

<sup>1</sup> Volen Center for Complex Systems, Brandeis University, Waltham, MA 02454, USA

<sup>2</sup> Stockholm Bioinformatics Center, Center for Physics, Astronomy, and Biotechnology, Stockholm 106 91, Sweden

<sup>3</sup> Dept. of Numerical Analysis and Computing Science, Royal Institute for Technology, Stockholm 100 44, Sweden

<sup>4</sup> Instituto de Neurociencias, Universidad Miguel Hernández-CSIC, San Juan de Alicante 03550, Spain

Received: 26 April 2002 / Accepted: 21 May 2002

**Abstract.** The concept of reverberation proposed by Lorente de Nó and Hebb is key to understanding strongly recurrent cortical networks. In particular, synaptic reverberation is now viewed as a likely mechanism for the active maintenance of working memory in the prefrontal cortex. Theoretically, this has spurred a debate as to how such a potentially explosive mechanism can provide stable working-memory function given the synaptic and cellular mechanisms at play in the cerebral cortex. We present here new evidence for the participation of NMDA receptors in the stabilization of persistent delay activity in a biophysical network model of conductance-based neurons. We show that the stability of working-memory function, and the required NMDA/AMPA ratio at recurrent excitatory synapses, depend on physiological properties of neurons and synaptic interactions, such as the time constants of excitation and inhibition, mutual inhibition between interneurons, differential NMDA receptor participation at excitatory projections to pyramidal neurons and interneurons, or the presence of slow intrinsic ion currents in pyramidal neurons. We review other mechanisms proposed to enhance the dynamical stability of synaptically generated attractor states of a reverberatory circuit. This recent work represents a necessary and significant step towards testing attractor network models by cortical electrophysiology.

## 1 Introduction

Reverberation refers to neural activity that circulates in a recurrent network. This concept was first developed in the 1930s by Lorente de Nó, whose systematic study of the vestibular–oculomotor reflex led him to postulate that neural after-discharges (responses that outlast a

brief stimulus for a fraction of a second) are produced by ‘self-reexcitation’ in closed chains of neurons (Lorente de Nó 1933, 1938a,b). Hebb proposed that the notion of reverberatory circuits has broad implications for cortical function: “To the extent that anatomical and physiological observations establish the possibility of reverberatory after-effects of a sensory event, it is established that such a process would be the physiological basis of a transient ‘memory’ of the stimulus” (Hebb 1949, p. 61). Hebb speculated that such a ‘transient memory’ trace could be maintained by reverberation in a cell assembly for an appreciable time, until the structural change of synapses is made for the formation of permanent memory.

Since the publication of Hebb’s influential book, Hebbian cell assemblies have been formulated and described mathematically in terms of attractor neural networks. The attractor theory was developed as a paradigm for associative long-term memory (e.g., Hopfield 1982), and for working memory (Amit 1995). ‘Working memory’ refers to an ‘immediate’ memory by which the brain actively holds and manipulates information online for a brief period of time (usually seconds). Because of its active nature, the neural process underlying this form of memory is manifestly observable. Indeed, in physiological studies, when an animal is required to remember a sensory cue across a delay between the stimulus and behavioral response, the maintenance of working memory during the delay period is correlated with elevated persistent neural activity in posterior parietal, inferotemporal, prefrontal, and other association cortices (Fuster 1995; Goldman-Rakic 1995). The attractor theory proposes that a stimulus-selective persistent neural firing pattern corresponds to a dynamically stable state that is self-sustained for a long time by excitatory reverberation in a recurrent circuit (Amari 1977; Amit 1995).

Milner (a former colleague of Hebb) criticized the attractor theory, on the grounds that a reverberatory neural assembly is ‘liable to fire out of control’ (Milner 1996). That is, positive feedback could drive neurons to fire at higher and higher rates until saturation is reached.

This would be inconsistent with the observation that mnemonic persistent activity in the cortex occurs at moderate rates (typically 10–50 Hz), significantly above the spontaneous firing rate (a few hertz), but well below the maximum firing capability of cortical neurons. When inhibition is incorporated to compensate for feedback excitation, ‘inhibitory damping might prevent reverberation altogether’ (Milner 1999). This problem of dynamical instability poses a serious challenge. It has not been investigated properly until recently when, with the advance in cortical physiology, it became possible for the first time to include realistic biophysical properties of cortical neurons and synapses in working-memory models (Amit and Brunel 1997; Lisman et al. 1998; Wang 1999; Compte et al. 2000; Durstewitz et al. 2000a; Brunel and Wang 2001). In particular, it was recognized that if the excitatory synaptic current is mediated by the AMPA receptors (AMPA), it would be significantly faster than feedback inhibition mediated by GABA<sub>A</sub> receptors. A strongly recurrent network with fast positive feedback/slow negative feedback is prone to instability. Either strong oscillations develop in a memory state or, worse, persistent activity is often disrupted in the middle of a delay period, thereby losing the memory (Wang 1999; Compte et al. 2000). Such instability could be prevented if the excitation is slow compared with negative feedback, i.e., when recurrent synapses are primarily mediated by the NMDA receptors (NMDARs) (Wang 1999; Compte et al. 2000). Moreover, the average synaptic excitation mediated by NMDARs is predicted to saturate at high neural firing rates, hence it is suitable for the rate control in memory states (Wang 1999).

Therefore, we suggested that both problems of the rate control and dynamical instability identified by Milner could be solved if the NMDA/AMPA ratio is sufficiently large at the recurrent synapses of a reverberatory network (Wang 1999; Compte et al. 2000; Wang 2001). This theoretical hypothesis, if proven correct, could have important implications for a critical role of the NMDARs in working memory, and for the theory of attractor networks in general (Wang 1999). However, one could ask: how large an NMDA/AMPA ratio is ‘sufficiently large’? How does the required NMDA/AMPA ratio depend on the details of the model, such as the relative excitatory and inhibitory current time courses or the synchronization properties of the network? Does it depend on the type of single neuron models used, such as the leaky integrate-and-fire (LIF) model versus the Hodgkin–Huxley-type conductance-based model? The present work was carried out to address these questions, using a conductance-based extension of our spatial working-memory model (Compte et al. 2000).

## 2 Methods

### 2.1 Neuron models

We have used a model of pyramidal neurons which have three compartments, representing a soma/initial axonal

segment (s), and proximal (d1) and distal (d2) dendrites. This architecture of single pyramidal cells is however not critical for the results presented here. The neuronal input–output relation and the shape of the somatic and dendritic action potential have been calibrated using cortical-slice data (McCormick et al. 1985; Markram et al. 1997). The membrane equations are

$$\begin{aligned} C_m \frac{dV_s}{dt} &= -I_{Na} - I_K - I_{Ca} - I_L - I_{Can} \\ &\quad - g_{c1}(V_s - V_{d1})/p_1 - I_{syn} \\ C_m \frac{dV_{d1}}{dt} &= -I_{Nap} - I_{KS} - I_L - g_{c1}(V_{d1} - V_s)/p_2 \\ &\quad - g_{c2}(V_{d1} - V_{d2})/p_2 - I_{syn} \\ C_m \frac{dV_{d2}}{dt} &= -I_A - I_{Ca} - I_L \\ &\quad - g_{c2}(V_{d2} - V_{d1})/(1 - p_1 - p_2) - I_{syn} \end{aligned}$$

with somatic voltage  $V_s$ , proximal dendritic voltage  $V_{d1}$ , and distal dendritic voltage  $V_{d2}$ , and where  $I_{Can}$  represents a cation current. Electrotonic parameter values are:  $g_{c1} = 0.75$ ,  $g_{c2} = 0.25$ ,  $p_1 = 0.5$ , and  $p_2 = 0.3$ . The calcium dynamics in the soma and the distal dendrite obey

$$\frac{d[Ca^{2+}]}{dt} = -\alpha I_{Ca} - [Ca^{2+}]/\tau_{Ca}$$

where (Wang 1998)

$$\begin{aligned} I_{Ca} &= g_{Ca} m_{\infty}^2(V)(V - E_{Ca}) \\ m_{\infty}(V) &= 1/(1 + \exp[-(V + 20)/9]) \\ E_{Ca} &= 120 \text{ mV} \end{aligned}$$

Somatic and distal dendritic parameters are:  $\alpha_s = 0.000667$ ,  $\alpha_{d2} = 0.002$  [in  $\mu\text{M}(\text{ms} \mu\text{A})^{-1} \text{cm}^2$ ],  $\tau_s = 240$  ms,  $\tau_{d2} = 80$  ms,  $g_{Ca} = 1.5$  (s), and  $g_{Ca} = 0.25$  (d2) (in  $\text{mS}/\text{cm}^2$ ).

Several of the ion conductances ( $I_{Can}$ ,  $I_{Na}$ ,  $I_{KS}$ , and  $I_A$ ) that have been identified in prefrontal pyramidal neurons are included in our cell model (Hammond and Crépel 1992; Fleidervish et al. 1996; Seamans et al. 1997). The slow cationic calcium-dependent current obeys

$$\begin{aligned} I_{Can} &= g_{Can} m^2(V - E_{Can}) \\ \frac{dm}{dt} &= \frac{m_{\infty}([Ca^{2+}]) - m}{\tau_{Can}([Ca^{2+}])} \\ m_{\infty}[Ca^{2+}] &= \frac{\alpha([Ca^{2+}])}{\alpha([Ca^{2+}]) + \beta} \\ E_{Can} &= -20 \text{ mV} \\ \beta &= 0.002 \text{ ms}^{-1} \\ \alpha &= 0.0056 [\text{ms}(\text{mM})]^{-1} \\ \tau_{Can}([Ca^{2+}]) &= \frac{1}{\alpha([Ca^{2+}]) + \beta} \text{ ms} \\ g_{Can} &= 0.025 \text{ mS}/\text{cm}^2. \end{aligned}$$

The proximal dendrite has a persistent sodium current which follows

$$I_{\text{Nap}} = g_{\text{Nap}} m_{\infty}^3 h (V - E_{\text{Nap}})$$

$$\frac{dh}{dt} = \alpha(V_{\text{d1}})(1 - h) - \beta(V_{\text{d1}})h$$

$$\alpha(V_{\text{d1}}) = 0.001 \exp[(-85 - V_{\text{d1}})/30]$$

$$\beta(V_{\text{d1}}) = \frac{0.0034}{\exp[(-17 - V_{\text{d1}})/10] + 1}$$

$$m_{\infty}(V_{\text{d1}}) = \frac{1}{1 + \exp[-(V_{\text{d1}} + 55.7)/7.7]}$$

$$g_{\text{Nap}} = 0.15 \text{ mS/cm}^2$$

and a slow potassium current which follows

$$I_{\text{KS}} = g_{\text{KS}} q r (V - E_{\text{KS}})$$

$$\frac{dq}{dt} = \frac{q_{\infty}(V_{\text{d1}}) - q}{\tau_q(V_{\text{d1}})}$$

$$q_{\infty}(V_{\text{d1}}) = \frac{1}{1 + \exp[-(V_{\text{d1}} + 34)/6.5]}$$

$$\tau_q(V_{\text{d1}}) = \frac{8}{\exp[-(V_{\text{d1}} + 55)/30] + \exp[(V_{\text{d1}} + 55)/30]}$$

$$\frac{dr}{dt} = \frac{r_{\infty}(V_{\text{d1}}) - r}{\tau_r(V_{\text{d1}})}$$

$$r_{\infty}(V_{\text{d1}}) = \frac{1}{1 + \exp[(V_{\text{d1}} + 65)/6.6]}$$

$$\tau_r(V_{\text{d1}}) = \frac{100}{1 + \exp[-(V_{\text{d1}} + 65)/6.8]} + 100$$

$$g_{\text{KS}} = 2.0 \text{ mS/cm}^2.$$

The A current in the distal dendrite obeys

$$I_{\text{A}} = g_{\text{A}} a^4 b (V - E_{\text{a}})$$

$$\frac{da}{dt} = \frac{a_{\infty}(V_{\text{d2}}) - a}{\tau_a(V_{\text{d2}})}$$

$$a_{\infty}(V_{\text{d2}}) = \frac{1}{1 + \exp[-(V_{\text{d2}} + 60)/8.5]}$$

$$\tau_a(V_{\text{d2}}) = 0.37$$

$$+ \frac{1}{\exp[(V_{\text{d2}} + 46)/5] + \exp[-(V_{\text{d2}} + 238)/37.5]}$$

$$\frac{db}{dt} = \frac{b_{\infty}(V_{\text{d2}}) - b}{\tau_b(V_{\text{d2}})}$$

$$b_{\infty}(V_{\text{d2}}) = \frac{1}{1 + \exp[(V_{\text{d2}} + 78)/6]}$$

$$\tau_b(V_{\text{d2}}) = 19$$

$$+ \frac{1}{\exp[(V_{\text{d2}} + 46)/5] + \exp[(V_{\text{d2}} + 238)/(-37.5)]}$$

$$g_{\text{A}} = 1.0 \text{ mS/cm}^2.$$

The model for the fast spiking interneuron includes sodium and potassium channels which reproduce neuronal input-output behavior (Wang and Buzsáki 1996).

## 2.2 Synapses

Synaptic currents are modeled as  $I_{\text{syn}} = g_{\text{syn}} s (V - E_{\text{syn}})$ , where  $g_{\text{syn}}$  is the maximal synaptic conductance, and  $E_{\text{syn}}$  (in millivolts) is the reversal potential ( $E_{\text{syn}} = 0$  for excitatory and  $E_{\text{syn}} = -70$  for inhibitory synapses). The gating variable  $s$  represents the fraction of open synaptic ion channels and follows first-order kinetics for AMPA and GABA transmission:

$$\frac{ds}{dt} = \alpha_s F(V_{\text{pre}})(1 - s) - s/\tau_s$$

where  $\alpha_s = 12 \text{ ms}^{-1}$ ,  $\tau_s = 2 \text{ ms}$  for AMPA, and inhibition decays as  $\tau_s = 10 \text{ ms}$  (Lisman et al. 1998). The normalized concentration of the postsynaptic transmitter-receptor complex,  $F(V_{\text{pre}})$ , is  $1/[1 + \exp(-V_{\text{pre}}/2)]$ . The voltage-dependent NMDA conductance introduces a multiplicative factor  $1/[1 + [\text{Mg}^{2+}] \exp(-0.062 V_{\text{m}})/3.57]$  (Jahr et al. 1990),  $[\text{Mg}^{2+}] = 1.0 \text{ mM}$ , into the synaptic equation. NMDA channels are represented by second-order kinetics as

$$\frac{dx}{dt} = \alpha_x F(V_{\text{pre}})(1 - x) - x/\tau_x$$

$$\frac{ds}{dt} = \alpha_s x(1 - s) - s/\tau_s$$

where  $x$  is a synaptic variable proportional to the neurotransmitter concentration in the synapse,  $\alpha_x = 10$ ,  $\tau_x = 2 \text{ ms}$ ,  $\alpha_s = 0.5$ , and  $\tau_s = 100 \text{ ms}$  (Wang 1999). No transmission delays were included in the model.

## 2.3 Network

The two population network model represents a local circuit of the dorsolateral prefrontal cortex in monkey. Pyramidal cells are four times more numerous than interneurons ( $N_{\text{E}} = 1024$ ,  $N_{\text{I}} = 256$ ). Neurons are spatially distributed in a ring according to the preferred cue stimulus in an oculomotor delayed response task, consistent with a columnar organization of the monkey prefrontal cortex (Goldman-Rakic 1995; Ó Scailidhe and Goldman-Rakic 1999; Rao et al. 1999; Constantinidis et al. 2001), and similar to models of the primary visual cortex (see, e.g., Ben-Yishai et al. 1995; Somers et al. 1995; Tsodyks and Sejnowski 1995). The strength of the recurrent connections between neurons in the network depends on the difference between their preferred cues. The conductance between neuron  $i$  and neuron  $j$  is described by  $g_{\text{syn},ij} = W(\theta_i - \theta_j) G_{\text{syn}}$ , where  $W(\theta_i - \theta_j)$  is the normalized ‘connectivity.’ The  $W$  for excitatory projections (pyramid-to-interneurons and pyramid-to-pyramid) is chosen as  $W(\theta_i - \theta_j) = J^- + (J^+ - J^-) \exp[-(\theta_i - \theta_j)^2/2\sigma^2]$  (Compte et al. 2000). The dimensionless parameter  $J^-$  represents the strength of the weak cross-directional connections,  $J^+$  the strength of the stronger isodirectional connections, and  $\sigma$  is the footprint of the connectivity.  $J^-$  is determined by normalization. We used  $J_{\text{EE}}^+ = 1.95$ ,  $J_{\text{EI}}^+ = 1.7$ , and  $\sigma_{\text{EE}} = \sigma_{\text{EI}} = 0.2$ , with the convention

that  $P_{XY}$  refers to the connection from X to Y for parameter  $P$ . Inhibitory projections are all to all (Fig. 1A shows a schematic diagram of the intracortical connectivity). For our reference parameter set, all the recurrent excitatory synaptic conductances were mediated exclusively by NMDA channels (Wang 1999). Our reference excitatory conductances are (in  $\text{mS}/\text{cm}^2$ )  $g_{EE} = 1.63$  and  $g_{EI} = 1.09$ , and the GABAergic inhibition is (in  $\text{mS}/\text{cm}^2$ )  $g_{IE} = 1.16$  and  $g_{II} = 0.65$ . All neurons receive external excitatory inputs mediated by AMPARs. This overall external input from other cortical areas is modeled as uncorrelated Poisson spike trains to each neuron at a rate of  $v_{\text{ext}} = 1000$  Hz per cell with the conductances  $g_{\text{ext},E} = 0.26$  and  $g_{\text{ext},I} = 0.06$  (in  $\text{mS}/\text{cm}^2$ ).

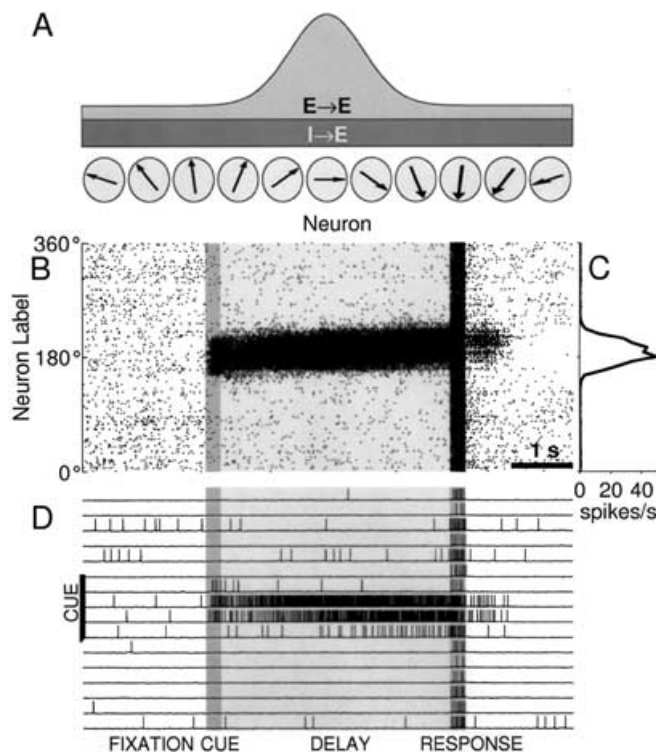


**Fig. 1A–D.** Working memory is maintained by a spatially localized sustained network activity state, a ‘bump attractor.’ **A** Schematic representation of the connectivity within the network. Excitatory ( $E$ ) cells receive strong excitation from neurons with similar preferred cue direction, and weaker excitation from those with dissimilar memory field. Inhibition ( $I$ ) to excitatory cells instead is nonspecific and arrives equally strongly from all interneurons in the network. **B** Activity profile during the delay period for the simulation in **C**. Since all neurons are identical, this curve is also the tuning curve for a neuron selective to location  $180^\circ$ . **C** Rastergram during a simulated visuospatial working-memory task. Each dot corresponds to an action potential from a pyramidal cell indexed by location  $y$  (labeled by the preferred cue  $0$ – $360^\circ$ ) at time  $x$ . Transient (250 ms,  $0.5 \mu\text{A}/\text{cm}^2$ ) cue presentation (indicated by bar) induces a tuned sustained memory state (delay period). Memory erasure is induced by a transient nonspecific current injection to all neurons (250 ms,  $0.8 \mu\text{A}/\text{cm}^2$ ). **D** Sample voltage traces from 16 equally spread ( $22.5^\circ$ ) pyramidal neurons

## 2.4 Simulation protocol

The simulation protocol was chosen to mimic the protocol used in the experiment of Funahashi et al. (1989), where monkeys were trained to fixate a central spot during a brief presentation (0.5 s) of a peripheral cue and throughout a subsequent delay period (1–6 s), and then to make a saccadic eye movement to where the cue had been presented in order to obtain a reward. We model the cue presentation to the network as a selective transient current injection (only during the cue period) to pyramidal cells with preferred cues close to the stimulus. A transient nonspecific current injection to all neurons produces a response at the end of the delay period.

## 2.5 Numerical integration

Code for the model simulation was written in C and the equations were integrated ( $\Delta t = 0.025$  ms) using a fourth-order Runge–Kutta algorithm (Press et al. 1992).

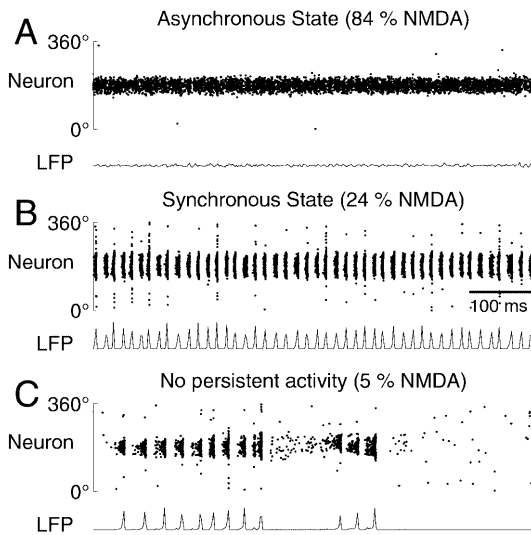
## 3 Results

Figure 1 shows a typical model simulation of the delayed oculomotor response experiment (Funahashi et al. 1989). Initially the network is in the resting state of unstructured spontaneous activity (0.5–1.5 Hz; Fig. 1C). A transient cue stimulus triggers the formation of a spatially localized activity pattern (a bump attractor) which outlasts the stimulus and persists through the delay period (Fig. 1B). The maximum firing rate of delay activity is moderate (40–50 Hz; Fig. 1B). Moreover, neurons fire asynchronously, and individual neurons show irregular spiking (Fig. 1D). Finally, a brief excitation recruits a surge of feedback inhibition from the interneuron population, the network is switched back to the spontaneous state, and the memory is erased. Thus, our conductance-based network model reproduces the findings of electrophysiological recordings in the dorsolateral prefrontal cortex of awake behaving monkeys during visuospatial working memory (Funahashi et al. 1989).

### 3.1 Synchronous and asynchronous working-memory modes

In the simulation shown by Fig. 1, recurrent synaptic excitation is mediated exclusively by NMDARs. Simulations with LIF neurons revealed that the asynchronous persistent state was destabilized when the NMDA/AMPA ratio at the recurrent synapses was reduced (Compte et al. 2000). We investigated whether this conclusion generalizes to the case when neurons are modeled by the Hodgkin–Huxley formalism. As in Compte et al. (2000), we gradually decreased the NMDA/AMPA ratio, while preserving the summated mean synaptic drive, and assessed how the network behavior is affected. We found

that a small reduction (16%) of the contribution from NMDARs is not sufficient to destabilize the asynchronous state (Fig. 2A). A further decrease of the NMDA/AMPA ratio leads to a different dynamical regime where the sustained mnemonic delay activity becomes synchronous (Fig. 2B). The pyramidal neuron population shows bands of activity that repeat rhythmically in time. The oscillation frequency increases with a shorter time constant of synaptic inhibition (Fig. 3). As the NMDAR component vanishes, spatially localized persistent activity becomes destabilized and disappears in the middle of the



**Fig. 2A–C.** The relative contribution from NMDA receptors (NMDARs) to the time integral (the charge) of a unitary excitatory postsynaptic current (EPSC) determines the temporal dynamics during the delay period. **A** Asynchronous delay firing when the contribution from NMDARs dominates. The lower trace represents the local field potential (LFP) calculated as the average of all synaptic activity in the network. **B** Increasing the synaptic AMPA receptor (AMPA) component induces synchronous but still stable delay-period activity. Notice the oscillatory pattern in the LFP (lower trace) at about 60 Hz. **C** Eventually, too much AMPAR component in intracortical excitation renders spatially tuned persistent activity unstable. These simulations were run with  $\tau_{\text{GABA}} = 4$  ms

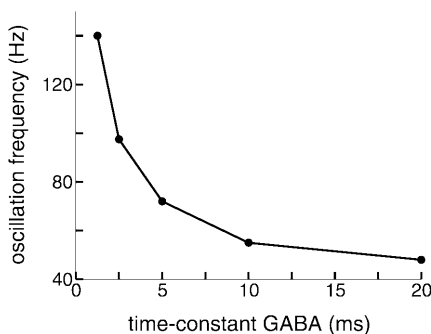


**Fig. 3.** The time constant of the inhibitory synaptic current determines the synchronized oscillation frequency. The oscillation frequency was estimated by the frequency of the peak in the power spectrum of the pyramidal population spiking activity (calculated with a timebase of 5 ms). Note that oscillations occur typically in the gamma (40- to 100-Hz) frequency range

delay period (Fig. 2C). This behavior is similar to what has been found in other studies using LIF neurons (Compte et al. 2000). When the NMDA/AMPA ratio is too small, the recurrent synaptic excitation dominated by AMPARs becomes too fast as compared with the time course of inhibition, the tuned delay activity becomes unstable, and a transient cue can therefore not be stored in the network.

Therefore, as the NMDA/AMPA ratio is reduced, the network behavior after a transient cue is successively transformed between three regimes: bump attractor with asynchronous firing (AS), bump attractor with synchronous firing (S), and a third regime in which no mnemonic activity (NM) could be elicited by the cue. To quantify and analyze the role of NMDARs in the dynamical stability of this reverberatory circuit, we set out to determine how the NMDA/AMPA ratios for the three behavioral regimes depend on the network properties.

### 3.2 Dependence on the inhibitory synaptic time constant and interneuron-to-interneuron connection

Intuitively, dynamical instability arises from a mismatch between the time constants of recurrent excitation and inhibition. The network should be more stable if feedback inhibition is faster. We tested this prediction by estimating how the critical amounts of NMDARs at the transitions  $\text{AS} \leftrightarrow \text{S}$  and  $\text{S} \leftrightarrow \text{NM}$  depend on the time constant  $\tau_{\text{GABA}}$  of the inhibitory synaptic current (Fig. 4). We measure the relative NMDAR contribution, (NMDA/(AMPA + NMDA)), as the ratio of the time integral of a unitary excitatory postsynaptic current when AMPARs are

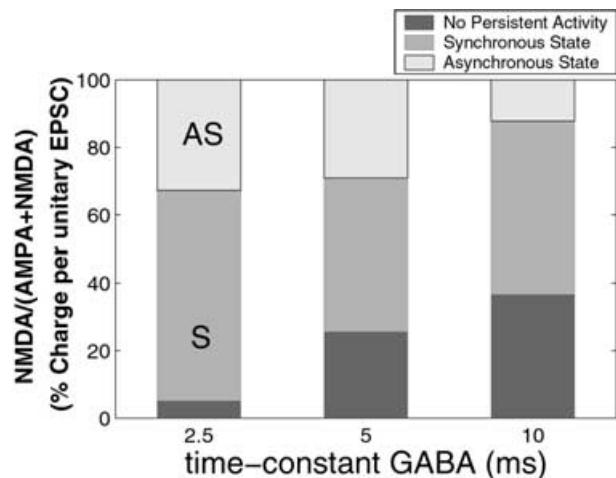


**Fig. 4.** The relative NMDAR contribution to recurrent excitation determines the dynamic mode of network behavior. At high NMDAR level, the spatially localized bump attractor is asynchronous. As the NMDAR component is decreased, the bump attractor becomes synchronous. Too little NMDAR contribution leads to the destabilization of the memory state (no persistent activity here means that the sustained firing did not last for more than 5 s). Note that faster inhibition (smaller  $\tau_{\text{GABA}}$ ) reduces the required NMDAR critical level significantly

blocked by the time integral of a composite unitary excitatory postsynaptic current mediated by both AMPARs and NMDARs. When the inhibitory time constant is 10 ms (reference value), the transition  $AS \leftrightarrow S$  occurs when the NMDAR contribution to recurrent excitation falls below 88%, and the transition  $S \leftrightarrow NM$  happens at 37% (Fig. 4). As expected, when inhibition is faster (with a shorter  $\tau_{GABA}$ ), the required NMDAR contribution for sustained delay activity is significantly reduced (Fig. 4). For example, with  $\tau_{GABA} = 2.5$  ms, NMDARs need to contribute only about 5% of the total charge, in order to sustain a stable (synchronous) spatially localized mnemonic state (transition  $S \leftrightarrow NM$ ). This is because the faster the inhibition, the shorter the period of the synchronized oscillations (Fig. 3). Therefore, less NMDAR-mediated slow excitation is needed to bridge across the silent time intervals between synchronized spikes. Moreover, the parameter range for the asynchronous memory state is also enlarged (transition  $AS \leftrightarrow S$  for 66% NMDA). Note that these simulations were performed with a fixed value of  $\tau_{AMPA} = 2$  ms. Our results show that when inhibition becomes as fast as excitation mediated by AMPARs (when the  $\tau_{AMPA}/\tau_{GABA}$  is sufficiently small), there is no longer a need for the slow NMDARs.

Furthermore, we observed that the network model is more susceptible to synchronous oscillations with a stronger inhibitory-to-inhibitory ( $g_{II}$ ) coupling. In fact, there is no longer an asynchronous state for any level of NMDAR contribution. Even when excitation is mediated exclusively by NMDARs, rhythmic bands appear in the delay period (Fig. 5). In this case, the inhibitory network receives a slow tonic drive from the pyramidal cell population, and oscillations are generated by mutual inhibition between interneurons (Wang and Buzsáki 1996; Traub et al. 1996). Progressive substitution of NMDARs for AMPARs further increases the synchronization during the oscillations until tuned persistent activity becomes dynamically unstable and the network enters the nonmnemonic (NM) regime. If a working-memory network operates in a more synchronous mode we would expect that a larger contribution of NMDARs is required in order to sustain the delay activity over the silent periods. Indeed, tuned synchronous delayed activity is abolished at a larger critical NMDAR component, 48% with a larger  $g_{II}$  value compared to 37% with a smaller  $g_{II}$  value ( $\tau_{GABA} = 10$  ms) (Fig. 5). This remains true for different values of  $\tau_{GABA}$  (Fig. 5). Hence, when the network is more synchronous due to an increased  $g_{II}$ , a larger amount of synaptic NMDAR component is required to ensure that the circuit can function as a working-memory circuit.

### 3.3 Differential effects of NMDARs in pyramidal cells and interneurons

In the simulations up to this point, we altered simultaneously the NMDA/AMPA ratio at all the excitatory connections. Now we assess the differential role of NMDARs in the excitatory connections onto pyramidal neurons ( $E \rightarrow E$ ) and those onto inhibitory fast-spiking

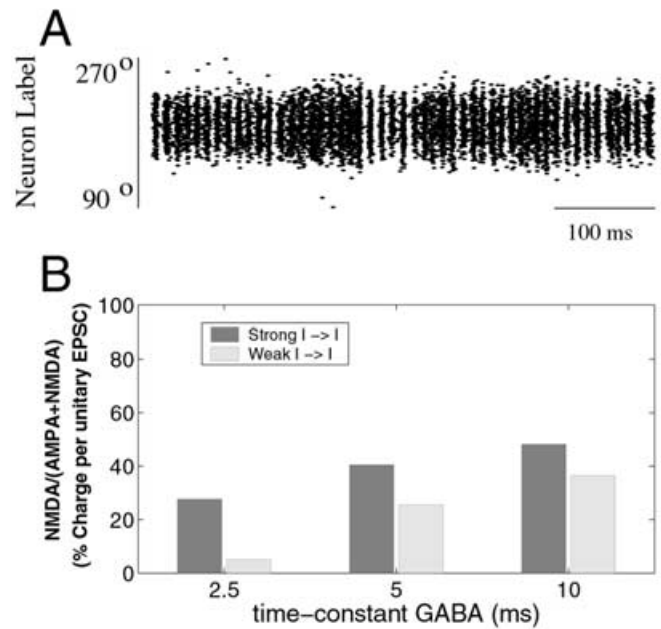


**Fig. 5A,B.** Strong interneuron-to-interneuron coupling renders the network more susceptible to oscillations and increases the critical amount of NMDA required for stable working-memory function. **A** Strong recurrent inhibition ( $g_{IE} = 1.93$ ,  $g_{II} = 1.09$ ) induces synchronous oscillations even though synaptic currents at recurrent excitatory synapses are entirely mediated by NMDARs. **B** Larger synaptic NMDA contribution is required for sustained delay firing when interneuron-to-interneuron coupling is strong. The critical NMDA ratios shown here correspond to the transition from synchronous tuned persistent activity to nonmnemonic function ( $S \leftrightarrow NM$  transition). Weak  $g_{II}$  corresponds to the reference case,  $g_{IE} = 1.16$  and  $g_{II} = 0.65$ , and strong  $g_{II}$  has the modified parameters  $g_{IE} = 1.93$  and  $g_{II} = 1.09$ .

neurons ( $E \rightarrow I$ ). We found that if we fix the NMDA level to either 100% or 50% at the  $E \rightarrow I$  connection, the stable mnemonic persistent state requires a much higher NMDA level at the  $E \rightarrow E$  connection when excitation to inhibitory cells is fully mediated by NMDARs (100%) than when it is partly (50%) mediated by AMPARs: the  $S \leftrightarrow NM$  transition occurs at 91% NMDA versus 48%, respectively, at the  $E \rightarrow E$  connection (Fig. 6). The network is more vulnerable when  $E \rightarrow I$  is mediated only by NMDARs because a tonically driven interneuronal network is prone to oscillations or/and because the excitation to the inhibitory population is not fast enough to allow inhibition to suppress the fast recurrent excitation of the pyramidal population mediated by AMPARs in the  $E \rightarrow E$  connections. If  $E \rightarrow I$  is 100% NMDA, the  $\tau_{GABA}$  value of the  $I \rightarrow E$  projection is no longer important.

The attractor dynamics is more stable if the NMDA/AMPA ratio at the  $E \rightarrow I$  projection is reduced, i.e., when the recruitment of feedback inhibition is more rapid. NMDAR-mediated excitation is slower than AMPAR-mediated synaptic transmission in bringing interneurons to threshold because of its slower rise time and possibly because of its saturation properties. This is one example where an increase in the synaptic NMDAR component (in  $E \rightarrow I$ ) can destabilize mnemonic activity.

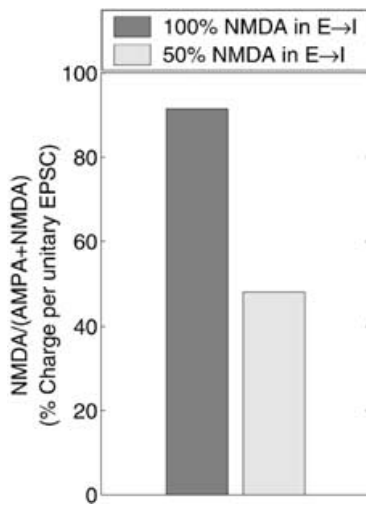


**Fig. 6.** The stabilizing effect of NMDARs depends on the type of synaptic connection. The critical level of NMDAR contribution to the E→E connection required for a stable memory state is much higher when the E→I connection is 100% NMDA than when it is 50% NMDA and 50% AMPA. Thus, the delay activity is most robust if there is a high level of NMDAR in the recurrent excitation, whereas the excitatory projections to the inhibitory population should be dominated by AMPAR ( $\tau_{\text{GABA}} = 10$  ms)

### 3.4 Slow intrinsic ionic current reduces the need for synaptic NMDAs

In the above simulations we focused on the synaptic interactions, and showed that NMDAR-mediated slow excitation is beneficial to network stability. We also tested the idea that intrinsic ion channels of single neurons could substitute the role of slow feedback excitation, so that the critical level of synaptic NMDAR contribution required for stable memory behavior is reduced. A slow calcium-dependent cation current has been identified in rat prefrontal neurons (Haj-Dahmane and Andrade 1998). We have calibrated the behavior of our neuron model using electrophysiological recordings from cortical slices (see Sect. 2). Figure 7A illustrates a typical voltage response to a current pulse when the isolated pyramidal neuron model includes an  $I_{\text{Can}}$  ionic current. Spike discharges cause a calcium influx which slowly activates the inward  $I_{\text{Can}}$  current. This produces a ramping-up time course of neuronal activity. Note after the current pulse the neuron displays after-discharges for hundreds of milliseconds, corresponding to the decay of  $I_{\text{Can}}$ . However, the neuron is not bistable for our reference parameter set, as it eventually returns to the resting state. In network simulations, if we remove the  $I_{\text{Can}}$  from pyramidal cells, the required critical level of NMDA is significantly increased (Fig. 7B). A small increase of the conductance  $g_{\text{Can}}$  further reduces the dependence on synaptic NMDAR component for the tuned mnemonic activity state. With further increase of the conductance  $g_{\text{Can}}$ , pyramidal neurons become intrinsically bistable (not shown). In this case, reverberation underlying memory behavior relies primarily on intrinsic cellular dynamics rather than on synaptic mechanisms. This regime will not be further elaborated

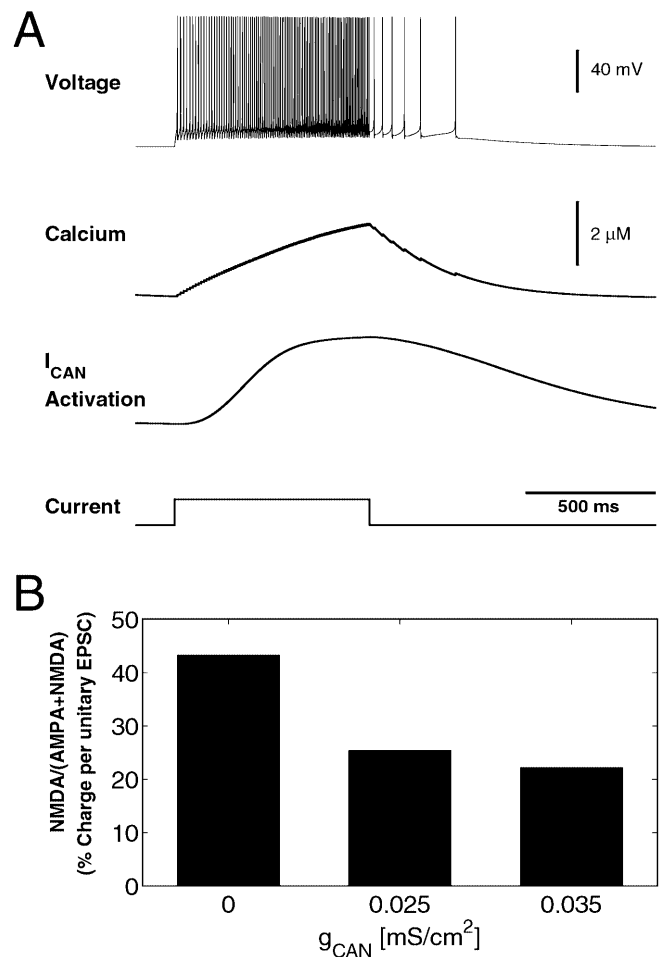


**Fig. 7.** **A** Electroresponsiveness of an isolated pyramidal cell model with a nonselective cation current  $I_{\text{Can}}$ . The calcium-dependent activation of  $I_{\text{Can}}$  is slow, leading to a ramping-up time course of the neural response. A few action potentials are still fired after stimulus extinction, in parallel with a slow deactivation of  $I_{\text{Can}}$ . Notice that the neuron is not bistable since it returns to a stable resting state. **B** Slow ionic currents (here  $I_{\text{Can}}$ ) reduce the critical level of NMDAR that is required for sustained delay activity. A further increase in  $g_{\text{Can}}$  renders the neuron intrinsically bistable and is therefore not included in this analysis of synaptically sustained network bistability

here, but will be reported elsewhere. We conclude that the critical amount of NMDA can be reduced, provided another slow feedback excitation mechanism is added to the circuit. Here this principle is exemplified in the form of a slow calcium-dependent ionic current, which is sufficiently weak so as not to induce intrinsic cellular bistability.

## 4 Discussion and relation to other work

### 4.1 NMDARs and stability of attractor working-memory models

The issue of the dynamical stability of synaptically sustained persistent states at physiological firing rates in networks of spiking neurons has been the focus of several recent research papers (Wang 1999; Compte et al. 2000;

Gutkin et al. 2001; Hansel and Mato 2001; Koulakov 2001; Laing and Chow 2001; Koulakov et al. 2002) and it has been discussed in two review papers (Durstewitz et al. 2000b; Wang 2001). All these studies found that synchronous firing during the persistent state was detrimental to its dynamical stability. This poses the synchrony problem for the stable maintenance of persistent activity: fast AMPAR-mediated recurrent excitation combined with the typically slower GABA<sub>A</sub> feedback inhibition will in general tend to synchronize the network activity, thus threatening the stability of persistent activity in the local circuit. Various possible (and mutually nonexclusive) mechanisms have been proposed to render persistent activity sustained by recurrent synaptic interactions dynamically stable, either by forcing asynchronous firing in the network or by inducing synchrony tolerance during persistent firing.

One such mechanism is the slow time course of NMDAR-mediated synaptic transmission. This was first proposed by Wang (1999) and then supported in other network simulations, both with LIF neurons (Compte et al. 2000; Koulakov 2001; Brunel and Wang 2001) and with conductance-based models (Durstewitz et al. 2000a; novel results reported here). Essentially, the idea is that to avoid the instability that arises from fast positive feedback and slow negative feedback, the excitatory feedback is made slower than the inhibitory feedback by replacing fast AMPAR-mediated transmission by slow NMDAR-mediated synaptic transmission. This substitution accomplishes two things: (i) asynchronous sustained activity is now possible because inhibitory feedback is no longer slower than excitatory feedback, and (ii) oscillatory sustained activity is stable to a certain degree because the long time constant of NMDARs bridges the intervals between successive oscillations of the excitatory population and makes self-sustained network firing possible. A sufficiently high level of synchrony will still destabilize the persistent state (Wang 1999; Compte et al. 2000; and Fig. 2 reported here). The results we report here, however, hint that this crucial role of NMDARs cannot be linked to a fixed NMDA level in recurrent excitation in prefrontal cortex. Indeed, the exact value of NMDA needed depends substantially on several factors, including the inhibitory synaptic time constant, strength of I-to-I connections, differential contribution of NMDA in E→E and E→I projections, and the presence of slow intrinsic membrane currents. It can be as low as 9% of the total excitatory charge and still be a crucial mechanism for the stability of memory function. Nevertheless, two qualitative conclusions are generally valid: (i) the larger is the NMDAR contribution to recurrent excitation, the more stable is a reverberatory network; and (ii) the required NMDA level is much higher for asynchronous than for synchronous persistent activity.

#### 4.2 Experimental tests

These studies give rise to questions that can be investigated experimentally. At the biophysical level, an

interesting question is the actual time constants of inhibitory synaptic currents in cortical neurons, or more importantly the ratio of  $\tau_{\text{AMPA}}/\tau_{\text{GABA}}$ . Measurements of this kind have been made for sensory neocortical areas (Xiang et al. 1998) and hippocampus (Xiang et al. 1998; Kraushaar and Jonas 2000; Bartos et al. 2001). Clearly, it would be useful to make a similar analysis for neurons of the prefrontal cortex. Another open question is the actual NMDA/AMPA ratio at recurrent prefrontal synapses.

On the other hand, the role of NMDARs could be investigated in physiological studies of behaving animals. For example, combining recording with iontophoresis of drugs in a delayed response experiment, it was found that delay-period activity was more effectively abolished by NMDAR antagonists than AMPAR antagonists in neurons of the premotor cortex (Fig. 8; Shima et al. 1998). This result supports a predominant role of NMDARs in delay-period activity.

Another issue of current debate is whether collective oscillations exist in persistent neural activity of the cortex during working memory. Pesaran et al. (2002) report clear evidence of gamma-band oscillations in the LFP of the lateral intraparietal cortex, especially during the delay period of an oculomotor delayed-response task. We have analyzed the spectral properties of prefrontal single units during a working-memory task (A. Compte,

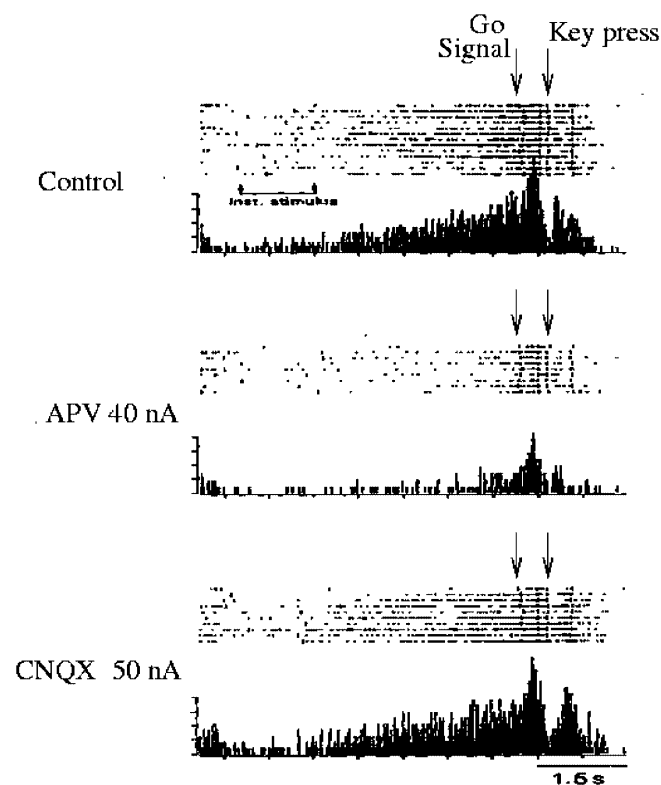


**Fig. 8.** Role of NMDARs and AMPARs in memory activity of a motor cortical neuron during a delayed-response task. Delayed-period activity (control, upper panel) is abolished by iontophoresis of the NMDAR antagonist APV (middle panel), but not by iontophoresis of the AMPAR antagonist CNQX (lower panel). In general, persistent activity was found to be more sensitive to NMDAR block than AMPAR block in this study. Data adapted with permission from Shima and Tanji (1998)

C. Constantinidis, J. Tegnér, S. Raghavachari, P. Goldman-Rakic, X.-J. Wang, unpublished work, 2002), and we have been unable to find oscillatory activity in individual spike trains, suggesting asynchronous collective firing. However, the crucial test is whether collective oscillations (as measured with LFP) are to be seen in prefrontal cortex during these tasks (as observed in the parietal cortex), and this is still an open question that has not yet been determined experimentally.

#### 4.3 Is NMDA necessary for biophysically realistic attractor networks?

Other mechanisms that do not depend on NMDARs have been proposed. Gutkin et al. (2001) show that a conductance-based neuron subject to a fluctuating synaptic input that barely depolarizes the neuron to its firing threshold triggers spikes with a variable finite delay with respect to the time its voltage crossed the threshold. This delay in firing is reportedly a mechanism to break the population synchrony that the interplay of AMPA and GABA<sub>A</sub> currents would generate. This effect does not exist in LIF neurons (where firing is instantaneous upon threshold crossing), and is not present in some other implementations of experimentally calibrated conductance-based cortical neurons (Durstewitz et al. 2000a); novel results presented here. This mechanism relies on a precise balance of excitation and inhibition, so that in the persistent state neurons are only driven above firing threshold by occasional fluctuations in the synaptic currents, causing a sizable delay to spike, so that the population activity is roughly asynchronous in the memory state. However, in the model of Gutkin et al. (2001) no realistic spontaneous activity is present in the resting state; and delay-period activity was typically simulated for only 500 ms during which time the bump state shows a large amount of drift. The stability of this model in more realistic conditions thus remains to be tested.

Another possible mechanism for solving the synchrony problem in the persistent state is strong interneuron-to-interneuron connections (Hansel and Mato 2001). By analytical methods, Hansel and Mato (2001) proved that strong mutual inhibition between inhibitory cells can help to stabilize an asynchronous state of persistent activity, even if excitatory feedback is only mediated by fast AMPARs. This result can be intuitively understood as follows. The oscillatory instability due to fast excitation/slow inhibition can be described by population activity (mean-field, or firing-rate) models (Wilson and Cowan 1973; Tsodyks et al. 1997; Wang 1999). An asynchronous state corresponds to a steady state of such a model, and the stability can be analyzed by equations linearized around the steady state:

$$\begin{aligned}\frac{dr_E}{dt} &= -r_E/\tau_E + w_{EE}r_E - w_{EI}r_I \\ \frac{dr_I}{dt} &= -r_I/\tau_I + w_{EI}r_E - w_{II}r_I\end{aligned}$$

where  $r_E$  and  $r_I$  are the excitatory and inhibitory population firing rates. It is apparent that the effective time constant  $\tau_{I,\text{eff}}$  for inhibition is given by  $1/\tau_{I,\text{eff}} = 1/\tau_I + w_{II}$ . Therefore, an increase in  $w_{II}$  (stronger I→I coupling) implies a reduction of  $\tau_{I,\text{eff}}$ , hence faster inhibition and better stability of the asynchronous state. Therefore, a certain level of interneuron-to-interneuron coupling could contribute to produce asynchronous persistent activity, perhaps in the absence of NMDARs. However, the results that we present here (Fig. 5B) raised the question of generality of this conclusion, since stronger I→I connection made our network more dependent on NMDARs. Several factors might explain the discrepancy between the two models. First, Hansel and Mato (2001) considered a discrete-population model with all-to-all coupling, whereas we studied a ring model with structured connectivity. The difference in the network's architecture could lead to different stability properties. Second, in the model of Hansel and Mato (2001) neurons receive little recurrent input and show no spontaneous activity in the resting state. By contrast, in our model neurons show spontaneous activity driven by massive background excitation and controlled by powerful feedback inhibition. The difference in the inhibition set point between the two models could underlie a distinct sensitivity to recurrent inhibition among interneurons. Finally, there is a second type of instability, produced by strong I→I interactions rather than by the excitatory–inhibitory loop (Traub et al. 1996; Wang and Buzsáki 1996). Thus, we expect that the I→I connection is beneficial to network stability only in a limited intermediate range of coupling strengths.

Finally, an additional mechanism that can provide extra stability to the memory behavior, even in the presence of synchronizations, is the existence of some kind of bistability at the synaptic level. Lisman et al. (1998) propose that the voltage dependence of NMDAR-type synaptic channels primes those synapses that are activated by the stimulus, and the network is shown to sustain stable, synchronized, persistent activity.

In summary, theoretical work has identified four mechanisms that can contribute to the stability of persistent activity sustained by synaptic reverberation. Two of them (participation of NMDARs and synaptic bistability) solve the problem by allowing the network to function in a stable manner in the presence of weak synchronization. To that end, slow mechanisms are introduced that bridge the gap between successive oscillatory episodes to maintain the reverberation in the network. The other two mechanisms (delayed spiking and self-inhibition of interneurons) help to stabilize an asynchronous persistent state. In principle, these candidate mechanisms can be tested experimentally in biophysical studies of cortical microcircuits and physiological studies of behaving animals.

#### 4.4 Instability in the location of the bump attractor

Our model for sustained delay activity in a spatial working-memory task is one example of a Mexican-

hat-type network (Amari 1977; Ben-Yishai et al. 1995; Camperi and Wang 1998; Pinto and Ermentrout 2001) for spatially localized activity. In this type of network (as opposed to architectures with distinct isolated populations: Amit and Brunel 1997; Brunel and Wang 2001; Durstewitz et al. 2000a), in addition to the dynamical instability discussed so far, another type of instability appears often. The localization of the bump of activity in one specific spot of the network can be unstable, and the bump can move systematically and indefinitely across the network. This property is detrimental to working-memory function, since the location of an initial cue cannot be read out from the location of the bump after the delay period. It has been shown that this effect is the result of *tuned* negative feedback on the excitatory population: local inhibitory feedback (Ben-Yishai et al. 1997) or activity-dependent outward currents in pyramidal neurons (Hansel and Sompolinsky 1998; Laing and Longtin 2001) both result in a moving bump. This is so because tuned negative feedback produces the largest hyperpolarizing current at the activity peak in the excitatory population. Hence, the profile drifts away from the strongest negative feedback, which in its turn keeps chasing the peak of activity in the network and pushing it continuously. In a network model of LIF neurons this phenomenon can be avoided by removing spike-frequency adaptation currents and by making feedback inhibition sufficiently broad (Compte et al. 2000). However, in a working-memory model of conductance-based neurons, even *unstructured* inhibitory connectivity produces *tuned* inhibition peaked at the center of the bump. The spatial tuning originates from the tuning in the driving force of the synaptic current. The pyramidal cells receive inhibition from inhibitory cells as  $I_I = g_I(V_E - E_{GABA})$ . Even if  $g_I$  is the same for all excitatory cells, the average membrane potential  $V_E$  is the largest for excitatory cells at the top of the bump, therefore inducing a structured spatial profile in the driving force ( $V_E - E_{GABA}$ ). In contrast, this phenomena does not occur for LIF neurons as the average membrane potential *decreases* with increased firing rate. Available data from cortical neurons (Anderson et al. 2000) suggest that the average potential increases with increasing firing, similar to conductance-based neuron models. This observation has two consequences:

1. It is more difficult to create a Mexican-hat type of connectivity (and a bump state) by using biophysical neurons. This difficulty can be overcome if inhibition comes from several different inhibitory populations (J. Tegnér, C. Constantinidis, P. Goldman-Rakic, X.-J. Wang, unpublished work, 2002), or limited by strong enough recurrent excitation (as shown here).
2. Once created, bumps will tend to drift continuously. Here, we noticed that this problem is less severe in the two-population model when there are slow inward currents ( $I_{Can}$ ) and no adaptation currents ( $I_{KCa}$ ) in the pyramidal cells. On the other hand, Laing and Longtin (2001) propose that neural noise can help to stabilize the location of a moving bump.

To further investigate the consequences of these phenomena under a variety of conditions it is important to use simplified models and mean field analysis of biophysical networks.

#### 4.5 Concluding remark

It would be interesting to carry out a systematic analysis of stability – and possible role of NMDARs – for other types of attractor network models endowed with realistic synaptic properties, ranging from recurrent models of primary visual cortex (Douglas et al. 1995; Somers et al. 1995; McLaughlin et al. 2000) to Hopfield-type associative memory models (Hopfield 1982). Further experimental and theoretical work in this direction will shed insights into the feasibility and dynamical operations of reverberatory neural networks à la Lorente de Nó and Hebb.

*Acknowledgements.* This work was supported by the National Science Foundation, the National Institutes of Health, and the Alfred P. Sloan Foundation (X.-J.W.). J.T. acknowledges support from the Wennergren Foundation, foundation for strategic research (SSF), Åke Wibergs foundation, Royal Academy of Science, and Fernströms Stiftelse.

#### References

- Amari S (1977) Dynamics of pattern formation in lateral-inhibition type neural fields. *Biol Cybern* 27: 77–87
- Amit DJ (1995) The Hebbian paradigm reintegrated: local reverberations as internal representations. *Behav Brain Sci* 18: 617
- Amit DJ, Brunel N (1997) Model of global spontaneous activity and local structured activity during delay periods in the cerebral cortex. *Cereb Cortex* 7: 237–252
- Anderson JS, Lampl I, Gillespie DC, Ferster D (2000) The contribution of noise to contrast invariance of orientation tuning in cat visual cortex. *Science* 290: 1968–1971
- Bartos M, Vida I, Frotscher M, Geiger JRP, Jonas P (2001) Rapid signaling at inhibitory synapses in a dendate gyrus interneuron network. *J Neurosci* 21: 2687–2698
- Ben-Yishai R, Lev Bar-Or R, Sompolinsky H (1995) Theory of orientation tuning in visual cortex. *Proc Natl Acad Sci USA* 92: 3844–3848
- Ben-Yishai R, Hansel D, Sompolinsky H (1997) Traveling waves and the processing of weakly tuned inputs in a cortical network module. *J Comput Neurosci* 4: 57–77
- Brunel N, Wang X-J (2001) Effects of neuromodulation in a cortical network model of object working memory dominated by recurrent inhibition. *J Comput Neurosci* 11: 63–85
- Camperi M, Wang X-J (1998) A model of visuospatial short-term memory in prefrontal cortex: recurrent network and cellular bistability. *J Comput Neurosci* 5: 383–405
- Compte A, Brunel N, Goldman-Rakic PS, Wang XJ (2000) Synaptic mechanisms and network dynamics underlying spatial working memory in a cortical network model. *Cereb Cortex* 10: 910–923
- Constantinidis C, Franowicz MN, Goldman-Rakic PS (2001) Coding specificity in cortical microcircuits: a multiple-electrode analysis of primate prefrontal cortex. *J Neurosci* 21: 3646–3655
- Douglas RJ, Koch C, Mahowald M, Martin KM, Suarez HH (1995) Recurrent excitation in neocortical circuits. *Science* 269: 981–985

- Durstewitz D, Seamans JK, Sejnowski TJ (2000a) Dopamine-mediated stabilization of delay-period activity in a network model of prefrontal cortex. *J Neurophysiol* 83: 1733–1750
- Durstewitz D, Seamans JK, Sejnowski TJ (2000b) Neurocomputational models of working memory. *Nat Neurosci* 3: 1184–1191
- Fleiderovich IA, Friedman A, Gutnick MJ (1996) Slow inactivation of  $\text{Na}^+$  current and slow cumulative spike adaptation in mouse and guinea-pig neocortical neurones in slices. *J Physiol (Lond)* 493: 83–97
- Funahashi S, Bruce CJ, Goldman-Rakic PS (1989) Mnemonic coding of visual space in the monkey's dorsolateral prefrontal cortex. *J Neurophysiol* 61: 331–349
- Fuster JM (1995) *Memory in the cerebral cortex*. MIT Press, Cambridge, Mass.
- Goldman-Rakic PS (1995) Cellular basis of working memory. *Neuron* 14: 477–485
- Gutkin BS, Laing CL, Colby CL, Chow CC, Ermentrout GB (2001) Turning on and off with excitation: the role of spiking timing asynchrony and synchrony in sustained neural activity. *J Comput Neurosci* 11: 121–134
- Haj-Dahmane S, Andrade R (1998) Ionic mechanism of the slow afterdepolarization induced by muscarinic receptor activation in rat prefrontal cortex. *J Neurophysiol* 80: 1197–1210
- Hammond C, Crépel F (1992) Evidence for a slowly inactivating  $\text{K}^+$  current in prefrontal cortical cells. *Eur J Neurosci* 4: 1087–1092
- Hansel D, Mato G (2001) Existence and stability of persistent states in large neuronal networks. *Phys Rev Lett* 86: 4175–4178
- Hansel D, Sompolinsky H (1998) Modeling feature selectivity in local cortical circuits. In: Koch C, Segev I (eds) *Methods in neuronal modeling*, 2nd edn. MIT Press, Cambridge, Mass.
- Hebb DO (1949) *The organization of behavior*. Wiley, New York
- Hopfield JJ (1982) Neural networks and physical systems with emergent collective computational abilities. *Proc Natl Acad Sci USA* 79: 2554–2558
- Jahr CE, Stevens CF (1990) Voltage dependence of NMDA-activated macroscopic conductances predicted by single-channel kinetics. *J Neurosci* 10: 3178–3182
- Koulakov A (2001) Properties of synaptic transmission and the global stability of delayed activity states. *Network* 12: 47–74
- Koulakov AA, Raghavachari S, Kepecs A, Lisman J (2002) Model for a robust neural integrator. *Nat Neurosci* 5: 775–782
- Kraushaar U, Jonas P (2000) Efficacy and stability of quantal GABA release at a hippocampal interneuron–principal neuron synapse. *J Neurosci* 20: 5594–5607
- Laing CR, Chow CC (2001) Stationary bumps in networks of spiking neurons. *Neural Comput* 13: 1473–1494
- Laing CR, Longtin A (2001) Noise-induced stabilization of bumps in systems with long-range spatial coupling. *Physica D* 160: 149–172
- Lisman JE, Fellous J-M, Wang X-J (1998) A role for NMDA-receptor channels in working memory. *Nat Neurosci* 1: 273–275
- Lorente de Nó R (1933) Vestibulo-ocular reflex arc. *Arch Neurol Psychiatry Chicago* 30: 245–291
- Lorente de Nó R (1938a) Analysis of the activity of the chains of internuncial neurons. *J Neurophysiol* 1: 207–244
- Lorente de Nó R (1938b) Synaptic stimulation of motoneurons as a local process. *J Neurophysiol* 1: 195–206
- Markram H, Lubke J, Frotscher M, Roth A, Sakmann B (1997) Physiology and anatomy of synaptic connections between thick tufted pyramidal neurones in the developing rat neocortex. *J Physiol (Lond)* 500: 409–440
- McCormick D, Connors B, Lighthall J, Prince D (1985) Comparative electrophysiology of pyramidal and sparsely spiny stellate neurons in the neocortex. *J Neurophysiol* 54: 782–806
- McLaughlin D, Shapley R, Shelley M, Wiesel DJ (2000) A neuronal network model of macaque primary visual cortex (V1): orientation selectivity and dynamics in the input layer 4C $\alpha$ . *Proc Natl Acad Sci USA* 97: 8087–8092
- Milner PM (1996) Neural representations: some old problems revisited. *J Cogn Neurosci* 8: 69–77
- Milner PM (1999) *The autonomous brain*. Erlbaum, Mahwah, N.J.
- Ó Scalaidhe SP, Goldman-Rakic PS (1999) Functional organization of prefrontal cortical columns in the macaque. *Soc Neurosci Abstr* 25: 620.2
- Pesaran B, Pezaris J, Sahani M, Mitra PP, Andersen RA (2002) Temporal structure in neuronal activity during working memory in macaque parietal cortex. *Nat Neurosci* 5: 805–811
- Pinto DJ, Ermentrout GB (2001) Spatially structured activity in synaptically coupled neuronal networks. II. lateral inhibition and standing pulses. *SIAM J Appl Math* 62: 226–243
- Press WH, Teukolsky SA, Vetterling WT, Flannery BP (1992) *Numerical recipes in C*. Cambridge University Press, Cambridge
- Rao SG, Williams GV, Goldman-Rakic PS (1999) Isodirectional tuning of adjacent interneurons and pyramidal cells during working memory: evidence for microcolumnar organization in PFC. *J Neurophysiol* 81: 1903–1916
- Seamans JK, Gorelova NA, Yang CR (1997) Contributions of voltage-gated  $\text{Ca}^{2+}$  channels in the proximal versus distal dendrites to synaptic integration in prefrontal cortical neurons. *J Neurosci* 17: 5936–5948
- Shima K, Tanji J (1998) Involvement of NMDA and non-NMDA receptors in the neuronal responses of the primary motor cortex to input from the supplementary motor area and somatosensory cortex: studies of task-performing monkeys. *Jpn J Physiol* 48: 275–290
- Somers DC, Nelson SB, Sur M (1995) An emergent model of orientation selectivity in cat visual cortical simple cells. *J Neurosci* 15: 5448–5465
- Traub RD, Whittington MA, Collins SB, Buzsáki G, Jefferys JGR (1996) Analysis of gamma rhythms in the rat hippocampus in vitro and in vivo. *J Physiol (Lond)* 493: 471–484
- Tsodyks MV, Sejnowski T (1995) Rapid state switching in balanced cortical network models. *Network* 6: 111–124
- Tsodyks MV, Skaggs WE, Sejnowski TJ, McNaughton BL (1997) Paradoxical effects of external modulation of inhibitory interneurons. *J Neurosci* 17: 4382–4388
- Wang X-J (1998) Calcium coding and adaptive temporal computation in cortical pyramidal neurons. *J Neurophysiol* 79: 1549–1566
- Wang X-J (1999) Synaptic basis of cortical persistent activity: the importance of NMDA receptors to working memory. *J Neurosci* 19: 9587–9603
- Wang X-J (2001) Synaptic reverberation underlying mnemonic persistent activity. *Trends Neurosci* 24: 455–463
- Wang XJ, Buzsáki G (1996) Gamma oscillation by synaptic inhibition in a hippocampal interneuronal network model. *J Neurosci* 16: 6402–6413
- Wilson HR, Cowan JD (1973) A mathematical theory of the functional dynamics of cortical and thalamic nervous tissue. *Kybernetik* 13: 55–80
- Xiang Z, Huguenard JR, Prince DA (1998) GABA<sub>A</sub> receptor-mediated currents in interneurons and pyramidal cells of rat visual cortex. *J Physiol (Lond)* 506: 715–730